

## Spectroscopic Properties of Sm<sup>3+</sup> Doped in Zinc Lithium Bismuth Borate Glasses

S.L. Meena

*Ceremic Laboratory, Department of physics,  
Jai Narain Vyas University, Jodhpur 342001(Raj.) India*

### Abstract

Glass sample of Zinc Lithium Bismuth Borate (25-x) Bi<sub>2</sub>O<sub>3</sub>:20Li<sub>2</sub>O:20ZnO:35 B<sub>2</sub>O<sub>3</sub>: x Sm<sub>2</sub>O<sub>3</sub>. (where x=1,1.5,2 mol%) have been prepared by melt-quenching technique. The amorphous nature of the prepared glass samples was confirmed by X-ray diffraction. FTIR spectra indicate that inclusion of TMI produces BO<sub>3</sub> and BO<sub>4</sub> structural units by breaking the boroxol (B<sub>2</sub>O<sub>6</sub>) ring. The absorption spectra of three Sm<sup>3+</sup> doped zinc lithium bismuth borate glasses have been recorded at room temperature. The various interaction parameters like Slater-Condon parameters F<sub>k</sub> (k=2,4,6), Lande parameters (ξ<sub>4F</sub>), nephelauxetic ratio (β'), bonding parameters (b<sup>1/2</sup>) and Racah parameters E<sup>k</sup> (k=1,2,3) have been computed. Judd-Ofelt intensity parameters and laser parameters have also been calculated.

**Keywords:** Zinc lithium bismuth borate glasses, Energy interaction parameters, Optical properties, Judd-Ofelt analysis.

### I. INTRODUCTION

The glass containing heavy metal oxide e.g. Bi<sub>2</sub>O<sub>3</sub> have attracted attention in recent years because of their wide range of applications in the field of glass ceramics, optical and optoelectronic devices [1-4]. Borate glasses can be a great hosts for a glass system because they can accommodate large concentrations of active ions and offer an important range of compositional possibilities such as metaborate, diborate, pentaborate, orthoborate and pyroborate. Glasses are important optical materials usually made to be transparent in the visible spectrum [5-7]. Among various glasses, borate glasses are excellent host matrices because boric oxide (B<sub>2</sub>O<sub>3</sub>) act as a good glass former and flux material [8]. Moreover bismuth oxide contained host glass

matrix improves chemical durability of the glass[9,10].For the linear properties(refractive index) this anionic group should act in similar way in an amorphous environment. Combining bismuth oxide with boric oxide thus allows tuning the optical properties in a wide range depending on the composition. Consequently the properties of glass of the system zinc lithium bismuth borate have attracted much interest [11, 12].

The aim of the present study is to prepare the  $\text{Sm}^{3+}$  doped zinc lithium bismuth borate glass with different  $\text{Sm}_2\text{O}_3$  concentrations. The absorption spectra, fluorescence spectra of  $\text{Sm}^{3+}$  of the glasses were investigated. The Judd-Ofelt theory has been applied to compute the intensity parameters  $\Omega_\lambda$  ( $\lambda=2, 4, 6$ ). These intensity parameter have been used to evaluate optical optical properties such as spontaneous emission probability, branching ratio, radiative life time and stimulated emission cross section. Large stimulated emission cross section is one of the most important parameters required for the design of high peak power solid state lasers.

## II. EXPERIMENTAL TECHNIQUES

### Preparation of glasses

The following  $\text{Sm}^{3+}$  doped bismuth borate glass samples (25-x)  $\text{Bi}_2\text{O}_3$ :20 $\text{Li}_2\text{O}$ :20 $\text{ZnO}$ :35  $\text{B}_2\text{O}_3$ : x  $\text{Sm}_2\text{O}_3$  (where x=1,1.5, 2) have been prepared by melt-quenching method. Analytical reagent grade chemical used in the present study consist of  $\text{Bi}_2\text{O}_3$ ,  $\text{Li}_2\text{O}$ ,  $\text{ZnO}$ ,  $\text{B}_2\text{O}_3$  and  $\text{Sm}_2\text{O}_3$ . They were thoroughly mixed by using an agate pestle mortar. then melted at 1060 $^\circ\text{C}$  by an electrical muffle furnace for 2h., After complete melting, the melts were quickly poured in to a preheated stainless steel mould and annealed at temperature of 360 $^\circ\text{C}$  for 2h to remove thermal strains and stresses. Every time fine powder of cerium oxide was used for polishing the samples. The glass samples so prepared were of good optical quality and were transparent. The chemical compositions of the glasses with the name of samples are summarized in Table 1.

**Table 1**

Chemical composition of the glasses

Sample	Glass composition (mol %)
ZnLiBiB (UD)	25 $\text{Bi}_2\text{O}_3$ :20 $\text{Li}_2\text{O}$ :20 $\text{ZnO}$ : 35 $\text{B}_2\text{O}_3$
ZnLiBiB (SM1)	24 $\text{Bi}_2\text{O}_3$ :20 $\text{Li}_2\text{O}$ :20 $\text{ZnO}$ : 35 $\text{B}_2\text{O}_3$ : 1 $\text{Sm}_2\text{O}_3$
ZnLiBiB (SM 1.5)	23.5 $\text{Bi}_2\text{O}_3$ :20 $\text{Li}_2\text{O}$ :20 $\text{ZnO}$ : 35 $\text{B}_2\text{O}_3$ : 1.5 $\text{Sm}_2\text{O}_3$
ZnLiBiB (SM 2)	23 $\text{Bi}_2\text{O}_3$ :20 $\text{Li}_2\text{O}$ :20 $\text{ZnO}$ : 35 $\text{B}_2\text{O}_3$ : 2 $\text{Sm}_2\text{O}_3$

ZnLiBiB (UD) -Represents undoped Zinc Lithium Bismuth Borate glass specimens

ZnLiBiB (SM) -Represents  $\text{Sm}^{3+}$  doped Zinc Lithium Bismuth Borate glass specimens

### III. THEORY

#### 3.1 Oscillator Strength

The intensity of spectral lines are expressed in terms of oscillator strengths using the relation [13].

$$f_{\text{expt.}} = 4.318 \times 10^{-9} \int \epsilon(\nu) d\nu \quad (1)$$

where,  $\epsilon(\nu)$  is molar absorption coefficient at a given energy  $\nu$  ( $\text{cm}^{-1}$ ), to be evaluated from Beer–Lambert law.

Under Gaussian Approximation, using Beer–Lambert law, the observed oscillator strengths of the absorption bands have been experimentally calculated [14], using the modified relation:

$$P_m = 4.6 \times 10^{-9} \times \frac{1}{cl} \log \frac{I_0}{I} \times \Delta\nu_{1/2} \quad (2)$$

where  $c$  is the molar concentration of the absorbing ion per unit volume,  $l$  is the optical path length,  $\log I_0/I$  is optical density and  $\Delta\nu_{1/2}$  is half band width.

#### 3.2. Judd-Ofelt Intensity Parameters

According to Judd [15] and Ofelt [16] theory, independently derived expression for the oscillator strength of the induced forced electric dipole transitions between an initial  $J$  manifold  $|4f^N(S, L) J\rangle$  level and the terminal  $J'$  manifold  $|4f^N(S', L') J'\rangle$  is given by:

$$\frac{8\pi^2 m c \bar{\nu}}{3h(2J+1)n} \frac{1}{n} \left[ \frac{(n^2+2)^2}{9} \right] \times S(J, J') \quad (3)$$

Where, the line strength  $S(J, J')$  is given by the equation

$$S(J, J') = e^2 \sum_{\lambda=2, 4, 6} \Omega_{\lambda} \langle 4f^N(S, L) J \| U^{(\lambda)} \| 4f^N(S', L') J' \rangle^2$$

In the above equation  $m$  is the mass of an electron,  $c$  is the velocity of light,  $\bar{\nu}$  is the wave number of the transition,  $h$  is Planck's constant,  $n$  is the refractive index,  $J$  and  $J'$  are the total angular momentum of the initial and final level respectively,  $\Omega_{\lambda}$  ( $\lambda = 2, 4, 6$ ) are known as Judd-Ofelt intensity parameters which contain the effect of the odd-symmetry crystal field terms, radial integrals and energy denominators.  $\|U^{(\lambda)}\|^2$  are the matrix elements of the doubly reduced unit tensor operator calculated in intermediate coupling approximation.  $\Omega_{\lambda}$  parameter can be obtained from least square fitting method [17] (Table 3). The matrix element  $\|U^{(\lambda)}\|^2$  that are insensitive to the environment of rare earth ions were taken from the literature [18].

### 3.3 Radiative Properties

The  $\Omega_\lambda$  parameters obtained using the absorption spectral results have been used to predict radiative properties such as spontaneous emission probability (A) and radiative life time ( $\tau_R$ ), and laser parameters like fluorescence branching ratio ( $\beta_R$ ) and stimulated emission cross section ( $\sigma_p$ ).

The spontaneous emission probability from initial manifold  $|4f^N(S', L') J' \rangle$  to a final manifold  $|4f^N(S, L) J \rangle$  is given by:

$$A[(S', L') J'; (S, L) J] = \frac{64 \pi^2 \nu^3}{3h(2J'+1)} \left[ \frac{n(n^2+2)^2}{9} \right] \times S(J', \bar{J}) \quad (4)$$

$$\text{Where, } S(J', J) = e^2 [\Omega_2 \|U^{(2)}\|^2 + \Omega_4 \|U^{(4)}\|^2 + \Omega_6 \|U^{(6)}\|^2]$$

The fluorescence branching ratio for the transitions originating from a specific initial manifold  $|4f^N(S', L') J' \rangle$  to a final manifold  $|4f^N(S, L) J \rangle$  is given by

$$\beta[(S', L') J'; (S, L) J] = \sum_{S L J} \frac{A[(S' L) J']}{A[(S' L') J' (\bar{S} \bar{L}) \bar{J}]} \quad (5)$$

where, the sum is over all terminal manifolds.

The radiative life time is given by

$$\tau_{rad} = \sum_{S L J} A[(S', L') J'; (S, L) J] = A_{Total}^{-1} \quad (6)$$

where, the sum is over all possible terminal manifolds. The stimulated emission cross-section for a transition from an initial manifold  $|4f^N(S', L') J' \rangle$  to a final manifold

$|4f^N(S, L) J \rangle$  is expressed as

$$\sigma_p(\lambda_p) = \left[ \frac{\lambda_p^4}{8\pi c n^2 \Delta\lambda_{eff}} \right] \times A[(S', L') J'; (\bar{S}, \bar{L}) \bar{J}] \quad (7)$$

where,  $\lambda_p$  the peak fluorescence wavelength of the emission band and  $\Delta\lambda_{eff}$  is the effective fluorescence line width.

### 3.4 Nephelauxetic Ratio ( $\beta$ ) and Bonding Parameter ( $b^{1/2}$ )

The nature of the R-O bond is known by the Nephelauxetic Ratio ( $\beta'$ ) and Bonding Parameters ( $b^{1/2}$ ), which are computed by using following formulae [19, 20]. The Nephelauxetic Ratio is given by

$$\beta' = \frac{\nu_g}{\nu_a} \quad (8)$$

where,  $\nu_a$  and  $\nu_g$  refer to the energies of the corresponding transition in the glass and free ion, respectively. The value of bonding parameter ( $b^{1/2}$ ) is given by

$$b^{1/2} = \left[ \frac{1-\beta'}{2} \right]^{1/2} \quad (9)$$

## IV. RESULT AND DISCUSSION

### 4.1 XRD Measurement

Figure 1 presents the XRD pattern of the sample contain -  $\text{B}_2\text{O}_3$  which is show no sharp Bragg's peak, but only a broad diffuse hump around low angle region. This is the clear indication of amorphous nature within the resolution limit of XRD instrument.

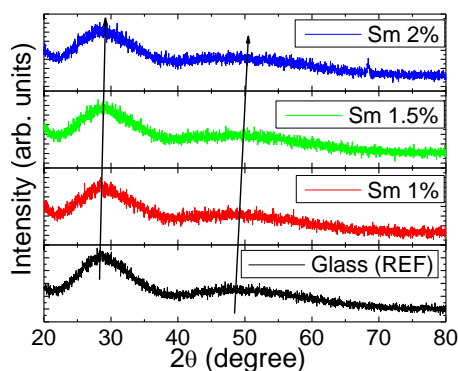


**Fig. 1:** X-ray diffraction pattern of  $\text{Bi}_2\text{O}_3$ :  $\text{Li}_2\text{O}$ :  $\text{ZnO}$ :  $\text{B}_2\text{O}_3$ :  $\text{Sm}_2\text{O}_3$

### 4.2. FTIR Transmission spectra

The FTIR spectra are presented in Fig.2 and the possible mechanism bands was tabulated in Table 2.

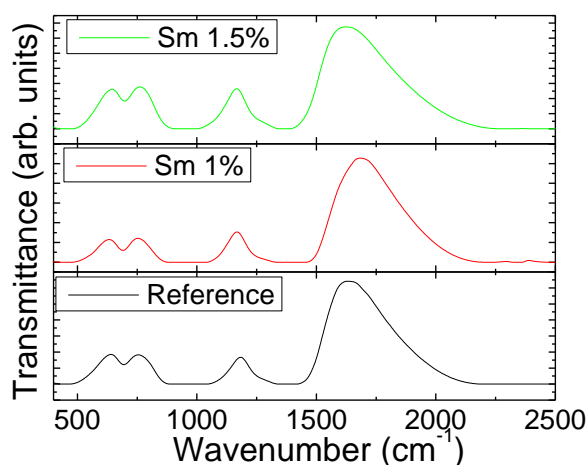


**Fig. 2:** IR transmission spectra for  $\text{Bi}_2\text{O}_3$ :  $\text{Li}_2\text{O}$ :  $\text{ZnO}$ :  $\text{B}_2\text{O}_3$ :  $\text{Sm}_2\text{O}_3$  glasses

The present set of glasses show very strong transmission bands in the region 470-525, 665-705, 990-1020, 1280-1360 and 2360-2500  $\text{cm}^{-1}$ . In borate glasses it has been reported that the bands observed in the region 470-525  $\text{cm}^{-1}$  are due to the variation metal cations such as  $\text{Zn}^{2+}$ . Whereas, the bands observed around 665-705  $\text{cm}^{-1}$  are due to the bending mode of B-O-B vibrations [21]. The bands observed in the range 990-1020  $\text{cm}^{-1}$  are assigned due to B-O bond stretching of the tetrahedral  $\text{BO}_4$  units. In the present glass system, the intermerging bands observed in the region 1280-1360  $\text{cm}^{-1}$

<sup>1</sup>are assigned to the asymmetric stretching of B-O bond in the trigonal units. The bands observed in the region 2360-2500 cm<sup>-1</sup> are due to hydroxol group [22].

**Table2.** Assignment of infrared transmission bands of sample glasses (ZnLiBiB SM)

Peak position(cm <sup>-1</sup> )	Assignment
470-525 (cm <sup>-1</sup> )	Varation metal cations such as Zn <sup>2+</sup>
665-705 (cm <sup>-1</sup> )	Bending of B-O-B linkage
990-1020 (cm <sup>-1</sup> )	B-O stretching of BO <sub>4</sub> tetrahedra
1280-1360 (cm <sup>-1</sup> )	Asymmetric stretching of B-O of trigonal
2360-2500 (cm <sup>-1</sup> )	Indication of OH groups

### 4.3 Absorption Spectrum

The absorption spectra of Sm<sup>3+</sup> doped ZnLiBiB(SM 01) glass specimen has been presented in Figure 3 in terms of optical density versus wavelength (nm). Ten absorption bands have been observed from the ground state <sup>6</sup>H<sub>5/2</sub> to excited states <sup>6</sup>F<sub>1/2</sub>, <sup>6</sup>F<sub>7/2</sub>, <sup>6</sup>F<sub>9/2</sub>, <sup>4</sup>G<sub>7/2</sub>, <sup>4</sup>I<sub>9/2</sub>, <sup>4</sup>M<sub>7/2</sub>, (<sup>6</sup>P, <sup>4</sup>P)<sub>5/2</sub>, <sup>4</sup>F<sub>7/2</sub>, <sup>4</sup>D<sub>1/2</sub>, and (<sup>4</sup>D, <sup>6</sup>P)<sub>5/2</sub> for Sm<sup>3+</sup> doped ZnLiBiB glasses.

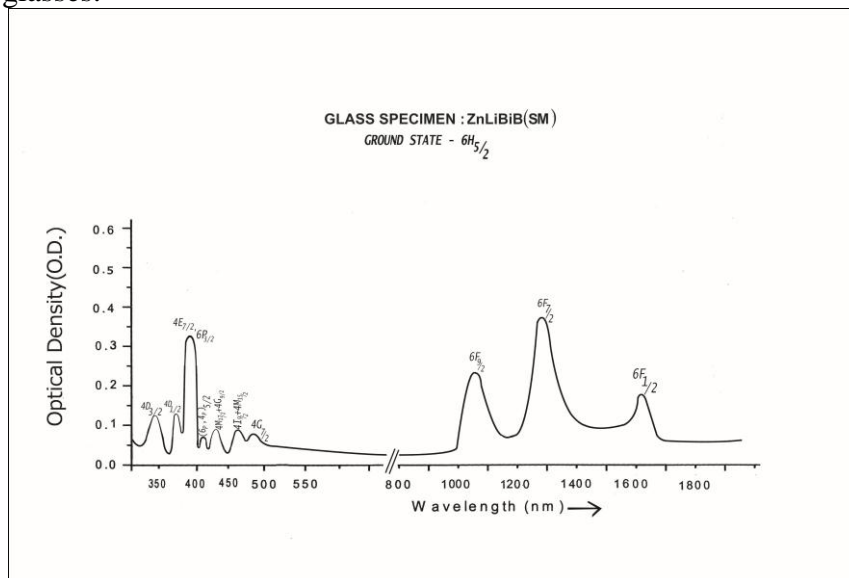


**Fig.3:** Absorption spectrum of Sm<sup>3+</sup>doped ZnLiBiB (01) glass

The experimental and calculated oscillator strengths for Sm<sup>3+</sup> ions in zinc lithium bismuth borate glasses are given in Table 3

**Table 3:** Measured and calculated oscillator strength ( $P_m \times 10^{+6}$ ) of Sm<sup>3+</sup> ions in ZnLiBiB glasses.

Energy level from <sup>6</sup> H <sub>5/2</sub>	Glass ZnLiBiB(SM01)		Glass ZnLiBiB(SM1.5)		Glass ZnLiBiB(SM02)	
	P <sub>exp.</sub>	P <sub>cal.</sub>	P <sub>exp.</sub>	P <sub>cal.</sub>	P <sub>exp.</sub>	P <sub>cal.</sub>
<sup>6</sup> F <sub>1/2</sub>	1.55	1.60	1.54	1.60	1.53	1.59
<sup>6</sup> F <sub>7/2</sub>	5.42	5.49	5.41	5.48	5.40	5.48
<sup>6</sup> F <sub>9/2</sub>	3.77	3.82	3.76	3.82	3.75	3.81
<sup>4</sup> G <sub>7/2</sub>	0.13	0.12	0.11	0.12	0.10	0.12
<sup>4</sup> I <sub>9/2</sub> , <sup>4</sup> M <sub>15/2</sub> , <sup>4</sup> I <sub>11/2</sub>	1.11	1.75	1.10	1.75	1.09	1.75
<sup>4</sup> M <sub>17/2</sub> , <sup>4</sup> G <sub>9/2</sub> , <sup>4</sup> I <sub>15/2</sub>	0.27	0.25	0.26	0.24	0.25	0.25
( <sup>6</sup> P, <sup>4</sup> P) <sub>5/2</sub> , <sup>4</sup> L <sub>13/2</sub>	1.30	1.30	1.20	1.29	1.26	1.29
<sup>4</sup> F <sub>7/2</sub> , <sup>6</sup> P <sub>3/2</sub> , <sup>4</sup> K <sub>11/2</sub>	5.52	5.58	5.51	5.57	5.50	5.57
<sup>4</sup> D <sub>1/2</sub> , <sup>6</sup> P <sub>7/2</sub> , <sup>4</sup> L <sub>17/2</sub>	2.39	2.42	2.38	2.42	2.37	2.41
<sup>4</sup> D <sub>3/2</sub> , ( <sup>4</sup> D, <sup>6</sup> P) <sub>5/2</sub>	2.42	3.44	2.40	3.44	2.30	3.43
r.m.s. deviation	±0.383		±0.393		±0.418	

Computed values of F<sub>2</sub>, Lande's parameter ( $\xi_{4f}$ ), Nephelauxetic ratio ( $\beta'$ ) and bonding parameter ( $b^{1/2}$ ) for Sm<sup>3+</sup> doped ZnLiBiB glass specimen are given in Table 4.

**Table 4.** F<sub>2</sub>,  $\xi_{4f}$ ,  $\beta'$  and  $b^{1/2}$  parameters for Samarium doped glass specimen.

Glass Specimen	F <sub>2</sub>	$\xi_{4f}$	$\beta'$	$b^{1/2}$
Sm <sup>3+</sup>	358.82	1258.16	0.9337	0.1821

Judd-Ofelt intensity parameters  $\Omega_\lambda$  ( $\lambda=2,4,6$ ) were calculated by using the fitting approximation of the experimental oscillator strengths to the calculated oscillator strengths with respect to their electric dipole contributions. In the present case the three  $\Omega_\lambda$  parameters follow the trend  $\Omega_2 > \Omega_4 > \Omega_6$ . The spectroscopic quality factor ( $\Omega_4/\Omega_6$ ) related with the rigidity of the glass system has been found to lie between 1.0903 and 1.0907 in the present glasses.

The value of Judd-Ofelt intensity parameters are given in **Table 5**

**Table 5:** Judd-Ofelt intensity parameters for Sm<sup>3+</sup> doped ZnLiBiB glass specimens

Glass Specimen	$\Omega_2(\text{pm}^2)$	$\Omega_4(\text{pm}^2)$	$\Omega_6(\text{pm}^2)$	$\Omega_4/\Omega_6$
ZnLiBiB(SM01)	4.154	3.853	3.534	1.0903
ZnLiBiB(SM1.5)	4.143	3.851	3.531	1.0906
ZnLiBiB(SM02)	4.115	3.838	3.519	1.0907

#### 4.4. Fluorescence Spectrum

The fluorescence spectrum of  $\text{Sm}^{3+}$  doped in zinc lithium bismuth borate glass is shown in Figure 4. There are four broad bands observed in the Fluorescence spectrum of  $\text{Sm}^{3+}$  doped zinc lithium bismuth borate glass. The wavelengths of these bands along with their assignments are given in Table 6. Fig. (4). Shows the fluorescence spectrum with four peaks ( ${}^4\text{G}_{5/2} \rightarrow {}^6\text{H}_{5/2}$ ), ( ${}^4\text{G}_{5/2} \rightarrow {}^6\text{H}_{7/2}$ ), ( ${}^4\text{G}_{5/2} \rightarrow {}^6\text{H}_{9/2}$ ) and ( ${}^4\text{G}_{5/2} \rightarrow {}^6\text{H}_{11/2}$ ), respectively for glass specimens.

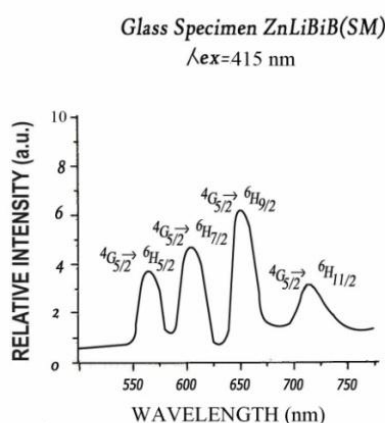


**Fig.4:** fluorescence spectrum of  $\text{Sm}^{3+}$  doped ZnLiBiB (01) glass

**Table 6.** Emission peak wave lengths ( $\lambda_p$ ), radiative transition probability ( $A_{\text{rad}}$ ), branching ratio ( $\beta$ ), stimulated emission cross-section ( $\sigma_p$ ) and radiative life time ( $\tau_R$ ) for various transitions in  $\text{Sm}^{3+}$  doped ZnLiBiB glasses

Transition	ZnLiBiB SM 01					ZnLiBiB SM 1.5				ZnLiBiB SM 02			
	$\lambda_{\text{max}}$ (nm)	$A_{\text{rad}}(\text{s}^{-1})$	$\beta$	$\sigma_p$ ( $10^{-20} \text{ cm}^2$ )	$\tau_R(\mu\text{s})$	$A_{\text{rad}}(\text{s}^{-1})$	$\beta$	$\sigma$ ( $10^{-20} \text{ cm}^2$ )	$\tau_R(\mu\text{s})$	$A_{\text{rad}}(\text{s}^{-1})$	$\beta$	$\sigma_p$ ( $10^{-20} \text{ cm}^2$ )	$\tau_R(\mu\text{s})$
${}^4\text{G}_{5/2} \rightarrow {}^6\text{H}_{5/2}$	563	13.227	0.0411	0.0040	3107.62	13.231	0.0411	0.0049	3107.49	13.218	0.0411	0.0052	3111.00
${}^4\text{G}_{5/2} \rightarrow {}^6\text{H}_{7/2}$	605	141.988	0.4412	0.0484		142.017	0.4413	0.0507		142.002	0.4418	0.0565	
${}^4\text{G}_{5/2} \rightarrow {}^6\text{H}_{9/2}$	655	132.083	0.4105	0.0461		132.035	0.4103	0.0479		131.705	0.4097	0.0502	
${}^4\text{G}_{5/2} \rightarrow {}^6\text{H}_{11/2}$	715	34.490	0.1072	0.0138		34.52	0.1073	0.0146		34.51	0.1074	0.0153	

#### V. CONCLUSION

In the present study, the glass samples of composition  $(25-x) \text{Bi}_2\text{O}_3:20\text{Li}_2\text{O}:20\text{ZnO}:35 \text{B}_2\text{O}_3: x \text{Sm}_2\text{O}_3$  (where  $x=1, 1.5, 2\text{mol} \%$ ) have been prepared by melt-quenching method. The Judd-Ofelt theory has been applied to calculate the oscillator strength

and intensity parameters  $\Omega_\lambda$  ( $\lambda=2, 4, 6$ ). The radiative transition probability, branching ratio are highest for ( $^4G_{5/2} \rightarrow ^6H_{7/2}$ ) transition and hence it is useful for laser action. The stimulated emission cross section ( $\sigma_p$ ) has highest value for the transition ( $^4G_{5/2} \rightarrow ^6H_{7/2}$ ) in all the glass specimens doped with  $Sm^{3+}$  ion. This shows that ( $^4G_{5/2} \rightarrow ^6H_{7/2}$ ) transition is most probable transition.

## REFERENCES

- [1] Rajesh,D., Balakrishna, A and Ratnakaram, Y.C.(2012).Luminescence, structural and dielectric properties of  $Sm^{3+}$  impurities in strontium lithium bismuth borate glasses. *Opt.Mat.* 35,108.
- [2] Gedam,R.S.,Ramteke, D.D.(2013). Influence of  $CeO_2$  addition on the electrical and optical properties of lithium borate glasses. *J.Phys. Chem.Solids*, 74, 1399.
- [3] Som,T. and Karmakar,B.(2008). Infrared-to-Red Upconversion Luminescence in Samarium-Doped Antimony Glasses.*J.of Luminescence*, 12, 1989.
- [4] Shen,L.F.,Chen,B.J.,Pun,Y.B. and Lin,H.(2015). $Sm^{3+}$  doped alkaline earth borate glasses as UV-Visible photon conversion for solar cells. *J.of Luminescence*, 160, 138.
- [5] Opera,I,Hesse,H.,Betzler,K.(2004).Optical properties of bismuth borate glasses.*Optical Materials*,26,235.
- [6] Agarwal,A.,Pal,I.,Sanghi,S.andAgarwal,M.P.(2009).Judd-Ofelt parameter and radiative Properties of  $Sm^{3+}$  ion doped zinc bismuth borate glasses,*Opt.mater*,32,399.
- [7] Sanghi,S.,Pal,I.,Agarwal,A. and Agarwal,M.P.(2011).Effect of  $Bi_2O_3$  on spectroscopic and structural properties of  $Er^{3+}$  doped cadmium bismuth borate glasses,*spectro.chema. acta*,83,94.
- [8] Wagh, A., Ajithkumar,M.P. and Kamath,S.D.(2013). Composition dependent structural and thermal properties of  $Sm_2O_3$  doped zinc fluoro borate glasses, *Energy research J.*4, 52.
- [9] Doualan, J.L.,Girard,S.,Haquin,H., and Adam,J.L.and Montagne, J. (2003).Spectroscopic properties and laser emission of  $Tm^{3+}$  doped ZBLAN glass at 1.8  $\mu m$ , *Optical Materials*, 24,563.
- [10]. Dumbaugh, W.H. and Lapp, J.C. (1992). Heavy-Metal Oxide Glass,*J. Am. Cer.Soc.*, 75,2315.
- [11] Alajerami, Y.S.M., Hashim,S.,Hassan, W.M.,Ramil, T.A.,Kasim,A.(2012).Optical properties of lithium magnesium borate glass doped with  $Dy^{3+}$  and  $Sm^{3+}$  ions,*Physics B: Condensed Matter*, 13,2398.

- [12] Rajesh, D., Naidu, M.D., Ratnakaram, Y.C. and Balakrishna, A. (2014). Ho<sup>3+</sup> doped strontium-aluminium-bismuth borate glasses for green light emission, *Luminescence*, 29, 854.
- [13]. Gorller-Walrand, C. and Binnemans, K. (1988) Spectral Intensities of f-f Transition. In: Gshneidner Jr., K.A. and Eyring, L., Eds., *Handbook on the Physics and Chemistry of Rare Earths*, Vol. 25, Chap. 167, North-Holland, Amsterdam, 101.
- [14]. Sharma, Y.K., Surana, S.S.L. and Singh, R.K. (2009) Spectroscopic Investigations and Luminescence Spectra of Sm<sup>3+</sup> Doped Soda Lime Silicate Glasses. *Journal of Rare Earths*, 27, 773.
- [15]. Judd, B.R. (1962). Optical Absorption Intensities of Rare Earth Ions. *Physical Review*, 127, 750.
- [16]. Ofelt, G.S. (1962) Intensities of Crystal Spectra of Rare Earth Ions. *The Journal of Chemical Physics*, 37, 511.
- [17]. Goublen, C.H. (1964). *Methods of Statistical Analysis*. Asian Publishing House, Bombay, Chap. 8, 138.
- [18]. Babu, P. and Jayasankar, C.K. (2001). Spectroscopy of Pr<sup>3+</sup> Ions in Lithium Borate and Lithium Fluoroborate Glasses. *Physica B: Condensed Matter*, 301, 326.
- [19]. Sinha, S.P. (1983). *Systematics and properties of lanthanides*, Reidel, Dordrecht.
- [20]. Krupke, W.F. (1974). *IEEE J. Quantum Electron* QE, 10, 450.
- [21] Coelho, J., Freire, C. and Huussain, N.S. (2012). Structural studies of lead lithium borate glasses doped with silver oxide, *Spectrochim. Acta A*, 86, 392.
- [22] Naresh, V. and Buddhudu, S. (2012). Structural, thermal, dielectric and ac conductivity properties of lithium fluoro-borate optical glasses. *Ceram. Int.*, 38, 2325.